

# Characterization of boron-doped diamond electrode by Raman spectroscopy with near infrared (785 nm) excitation

**Gediminas Niaura\***,

**Romas Ragauskas,**

**Arvydas Dikčius,**

**Benjaminas Šebeka,**

**Zenonas Kuodis**

*Institute of Chemistry,  
A. Goštauto 9,  
LT-01108 Vilnius,  
Lithuania*

The boron-doped diamond (BDD) electrode has been characterized by ordinary Raman and surface-enhanced Raman spectroscopy using a 785-nm excitation. A relative enhancement of  $sp^3$ -carbon bands associated with amorphous (disordered) diamond at 1180 and 1272  $cm^{-1}$  was observed in the 785-nm spectrum versus the crystalline diamond band at 1327  $cm^{-1}$ . In addition, frequency downshift of amorphous and crystalline diamond bands was established. In contrast to 532 and 632.8 nm excited spectra, no  $sp^2$ -like bands of amorphous carbon (D and G bands) were detected with near-infrared (NIR) excitation. The observed changes were interpreted assuming an increase in the probing depth of the Raman experiment with a longer wavelength and resonance enhancement of larger amorphous diamond clusters. It has been demonstrated that BDD electrode surface carbon structures can be effectively probed by the NIR SERS approach using Au nanoparticles prepared by the hot citrate reduction method.

**Key words:** boron-doped diamond, Raman, NIR excitation, 785 nm, SERS

## INTRODUCTION

Boron-doped diamond (BDD) films have been recognized as a material highly suitable for electrochemical applications such as wastewater treatment, oxidation of organic compounds, electroanalysis, and electrosynthesis because of its chemical inertness, mechanical hardness, and a wide potential window [1–3]. The electrochemical properties of BDD electrode depend on the doping level, diamond content, purity and structure of the film [3]. Useful information on the structure and purity of diamond films can be collected by Raman spectroscopy [4, 5].

It was demonstrated that shifting the excitation wavelength from the red spectral region to a blue and even a UV range dramatically increases the relative intensity of  $sp^3$ -carbon as compared with  $sp^2$ -bonded species [6]. Thus, detailed molecular-level information on different carbon structures and defects can be acquired from Raman experiments performed at several excitation wavelengths. Whereas Raman spectroscopy with visible excitation was widely applied for the characterization of diamond films, few works have been reported on the Raman study of BDD electrodes using near-infrared excitation, in particular the 785 nm laser line [4, 6].

The aim of the present study was to show the advantages and limitations of Raman spectroscopy for the characterization of BDD films using the 785 nm excitation in comparison with the visible (532 and 633 nm) approach.

## EXPERIMENTAL

The BDD electrode (size 12 × 12 mm) was purchased from the Swiss Center for Electronics and Microtechnology (SA Neuchatel, Switzerland). The electrode substrate was made from monocrystalline silicon, resistivity 10–20  $M\Omega$  cm. The Ti–Au layer (1  $\mu m$ ) was used for backside metallization, and the boron-doped diamond layer (1000 ppm boron) was 1.2  $\mu m$  thick. The Millipore purified water was used throughout the experiments. Sodium citrate, inorganic acids and salts,  $H AuCl_4 \cdot 3H_2O$  (ASC reagent grade) were purchased from Sigma-Aldrich Chemie GmbH and used without further purification.

Near-infrared Raman spectra were recorded using an Echelle type RamanFlex 400 spectrometer (Perkin–Elmer, Inc.) equipped with a thermoelectrically cooled ( $-50$  °C) CCD camera and a fiber-optic cable for the excitation and collection of the Raman spectra. The 785-nm beam of the diode laser was used as the excitation source. The 180° scattering geometry was employed. The laser power at the sample was restricted to

\* Corresponding author. E-mail: gnaiura@ktl.mii.lt

20 mW, and the beam was focused to a 200  $\mu\text{m}$  diameter spot on the electrode. The integration time was 10 s. Each spectrum was recorded by accumulation of 50 scans. In order to increase the signal-to-noise ratio, four spectra were averaged. The Raman frequencies were calibrated using the polystyrene standard (ASTM E 1840) spectrum. The intensities were calibrated by the NIST intensity standard (SRM 2241).

632.8-nm excited spectra were recorded with a Horiba Jobin Yvon spectrometer LabRam HR800 equipped with a 1800 groove / mm grating. The He-Ne laser power at the sample was adjusted to 3 mW. Raman spectra were taken by using 100 $\times$  / 0.90 NA objective lens. The spectra were calibrated using the Si band at 520.6  $\text{cm}^{-1}$ . The integration time was 600 s and the spectral resolution was 0.8  $\text{cm}^{-1}$  in the vicinity of 1370  $\text{cm}^{-1}$ .

532-nm excited Raman spectra were recorded using a 500 mm focal length,  $f / 6.4$  aperture ratio spectrograph (Acton Research Co., Model: SpectraPro-2500i) equipped with 1200 lines / mm grating and a thermoelectrically cooled ( $-60\text{ }^\circ\text{C}$ ) CCD camera (Princeton Instruments, Model: Spec-10: 256E). A diode-pumped solid-state laser (Viasho Technologies Co. Ltd.) was used as the excitation source. The incidence angle of the laser beam was  $60^\circ$  and the laser power at the sample was typically 10 mW. Experiments were carried out in  $90^\circ$  geometry. A long wave pass edge filter (Semrock, Inc.) was placed in front of the entrance slit of the spectrograph to eliminate Rayleigh scattering from the sample. The Raman frequencies were calibrated using the toluene spectrum. The integration time was 1 s. Each spectrum was recorded by accumulation of 300 scans. In order to reduce photo- and thermoeffects, the sample was moved linearly with respect to the laser beam at a rate of about 20 mm/s [7].

Au nanoparticles for SERS experiments were prepared by the citrate thermal reduction method [8]; 50 mL solution containing  $5 \times 10^{-4}$  M of  $\text{HAuCl}_4 \cdot 3\text{H}_2\text{O}$  was heated to its boiling point; 2.6 mL of 1% sodium citrate solution was added to the boiling solution while continuously stirring. The reaction was completed after about 15 min, and the color of the solution turned to wine red. The electronic absorption spectrum of Au colloidal solution showed its maximum at 519 nm. Nanoparticles were stable at least several months. The 20  $\mu\text{L}$  drop of Au sols was placed on the substrate under investigation, and the water was evaporated. To remove the adsorbed citrate ions and oxidation products, the aggregate colloidal particles at the surface were carefully washed by placing a 100  $\mu\text{L}$  drop of water for 5 min. After that the water was removed by using a pipette. Such a procedure was repeated five times, and finally the residual water was evaporated. The concentration of Au nanoparticles at the surface decreases after such procedure; however, the observed SERS spectrum is relatively free from the citrate bands or other adsorbate spectral features.

## RESULTS AND DISCUSSION

An overview of the Raman spectrum of the BDD film obtained using a 785-nm excitation is displayed in Fig. 1. The most intense and narrow peak at 520.6  $\text{cm}^{-1}$ , along with weaker features near 303 and 940  $\text{cm}^{-1}$ , belong to the vibrational modes of silicon substrate. Presence of a crystalline diamond in the film is visible from the characteristic band at 1328  $\text{cm}^{-1}$  [4, 5, 9]. In the following, we will focus on the narrow spectral region (1000–1700  $\text{cm}^{-1}$ ) where vibrations of various carbon structures take place. Figure 2 compares the Raman spectra of the same BDD electrode obtained using the 532, 633, and 785 nm excitation wavelengths. Experimental spectra were fitted with mixed Gaussian-Lorentzian form components. Table summarizes the parameters and assignments [4, 5, 10–17] of the fitted curve constituents. Presence of boron in the film is evidenced by the broad bands near 1165–1200 and 1272–1298  $\text{cm}^{-1}$ . These features were assigned to the phonon density of states (PDOS) of diamond bands that appeared due to a boron-induced relaxation of selection rule [13–16]. The broad features at 1368 and 1565–1568  $\text{cm}^{-1}$  are associated with G and D bands, respectively, of graphitic carbon [4, 5]. The  $\text{sp}^2$  carbon at grain boundaries was assigned to the 1447–1479  $\text{cm}^{-1}$  band [4, 10, 11, 15]. The weak feature near 1087  $\text{cm}^{-1}$  was tentatively attributed to vibrations of diamond nanocrystallites ( $\text{sp}^3$  carbon) [10, 12].

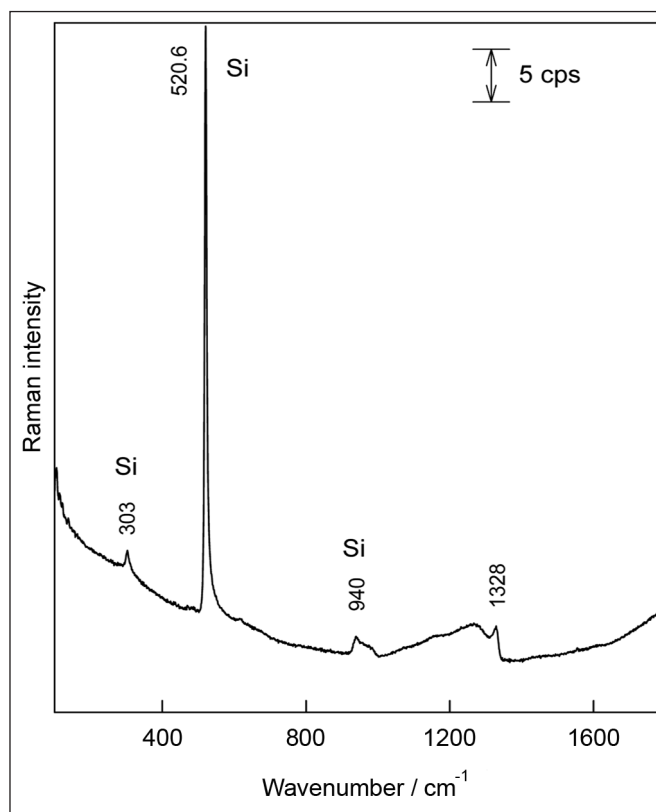


Fig. 1. Overview of Raman spectrum of the BDD electrode. Experimental conditions: integration time 2000 s, excitation 785 nm, 20 mW

Table. Frequencies ( $\text{cm}^{-1}$ ), normalized integrated intensities (arb. un.)<sup>a</sup> and assignments of fitted contour components obtained with different laser excitation wavelengths

$\lambda_{\text{ex}} = 532 \text{ nm}$	$\lambda_{\text{ex}} = 632.8 \text{ nm}$	$\lambda_{\text{ex}} = 785 \text{ nm}$	Assignments	References
–	1076 (51)	–	$\text{sp}^2$ carbon, trans-polyacetylene laying in the grain boundaries <sup>b</sup>	10, 11
–	–	1087 (186)	$\text{sp}^3$ carbon, diamond nanocrystallites <sup>b</sup>	10, 12
1165 (138)	1200 (487)	1180 (716)	$\text{sp}^3$ carbon, amorphous, disordered diamond, PDOS-band (X point), appeared because of the boron induced relaxation of selection rule associated with wave vector	13, 14
1298 (164)	1298 (329)	1272 (743)	$\text{sp}^3$ carbon, amorphous, disordered diamond, PDOS-band (L point), appeared because of the boron induced relaxation of selection rule associated with wave vector	13–16
1330.9 (100)	1331.2 (100)	1326.8 (100)	$\text{sp}^3$ carbon, first-order peak of crystalline diamond	4, 5, 13, 17
1368 (202)	1368 (105)	–	$\text{sp}^2$ carbon, D-band of amorphous carbon	4, 5
1479 (266)	1447 (418)	–	$\text{sp}^2$ carbon, trans-polyacetylene laying in the grain boundaries <sup>b</sup>	4, 10, 11, 15
1565 (107)	1568 (234)	–	$\text{sp}^2$ carbon, G-band of amorphous carbon	4, 5

<sup>a</sup>In parentheses, <sup>b</sup>debatable assignment. Abbreviations: PDOS, phonon density of states of diamond.

Several useful characteristics of BDD film might be derived from the analysis of relative intensities in the Raman spectra. Figure 2 clearly shows that the relative intensity of the crystalline diamond ( $1327\text{--}1331 \text{ cm}^{-1}$ ) and non-diamond bands (Table) depends on the excitation wavelength. Based on analysis of  $514.5 \text{ nm}$ -excited spectra, it was demonstrated previously that the Raman cross-section of the diamond band is  $\sim 50$  times lower as compared with  $\text{sp}^2$ -carbon [9]. Thus, the relative content of diamond in the film, i. e. diamond purity, can be evaluated by the analysis of the integrated intensities of diamond ( $A_{\text{diamond}}$ ) and non-diamond ( $A_{\text{non-diamond}}$ ) peaks from the area of fitted curves (Table 1) of the  $532 \text{ nm}$ -excited spectrum by using the relation [18, 19]:

$$C_{\text{diamond}} = \frac{100 A_{\text{diamond}}}{\left( A_{\text{diamond}} + \frac{\sum A_{\text{non-diamond}}}{50} \right)} \quad (1)$$

According to this procedure, the diamond content in the BDD film studied was found to be 90%. In the estimation of diamond purity, we analyzed only the crystalline diamond  $1332 \text{ cm}^{-1}$  peak and amorphous carbon bands at  $1368$ ,  $1447$ , and  $1568 \text{ cm}^{-1}$ . One of the reasons for an increased amount of graphitic material is presence of boron atoms.

The D / G band intensity ratio and the width of the G band were used to measure the particle size of graphitic carbon in the diamond films [5]. The amorphous carbon D and G bands are visible in both  $532 \text{ nm}$ - and  $632.8 \text{ nm}$ -excited spectra. However, the signal-to-noise ratio is higher for the Raman spectrum obtained using red excitation. The peak intensity ratio  $I_{\text{D}} / I_{\text{G}}$ , in this case determined from the fitted components, was found to be 0.86,

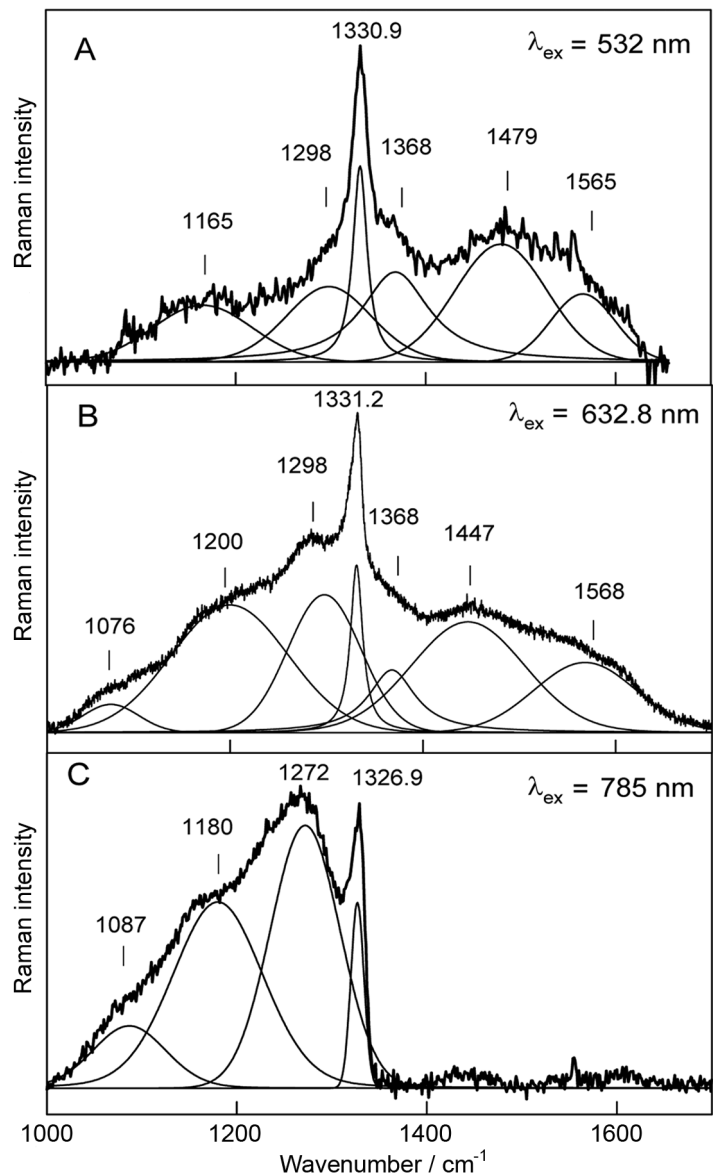


Fig. 2. Raman spectra of BDD electrode obtained using (A)  $532 \text{ nm}$ , (B)  $632.8 \text{ nm}$ , and (C)  $785 \text{ nm}$  excitation wavelengths with added Lorentzian–Gaussian form curve fitting

yielding an approximate particle size near 51 Å. Such relatively small dimensions of the graphitic carbon particles correlate well with the high FWHM value ( $125\text{ cm}^{-1}$ ) of the G peak.

The spectrum excited with the 785 nm laser line differs completely from 532 nm- and 632.8 nm-excited spectra. The bands of amorphous carbon (near  $1368$  and  $1568\text{ cm}^{-1}$ ) and the broad feature due to  $\text{sp}^2$ -carbon at grain boundaries (near  $1447\text{ cm}^{-1}$ ) cannot be detected with the 785 nm excitation. Instead, lower frequency components due to boron-induced PDOS bands (near  $1180\text{ cm}^{-1}$  and  $1272\text{ cm}^{-1}$ ) and nanocrystalline diamond (at  $1087\text{ cm}^{-1}$ ) are considerably enhanced. It should be noted that all enhanced bands are related to  $\text{sp}^3$ -carbon (probably amorphous diamond) structures (Table). The relative intensity of amorphous diamond ( $A_{\text{amorphous-d}} / A_{\text{crystalline-d}}$ ), determined from the integrated areas of the band near  $1298\text{--}1274\text{ cm}^{-1}$  ( $A_{\text{amorphous-d}}$ ) and the crystalline diamond band at  $1327\text{--}1331\text{ cm}^{-1}$  ( $A_{\text{crystalline-d}}$ ), increases with increasing excitation wavelength in the order:

$$1.6 (532\text{ nm}) < 3.3 (632.8\text{ nm}) < 7.4 (785\text{ nm}). \quad (2)$$

It should be noted that not only the relative Raman intensities but also the positions of the components are sensitive to  $\lambda_{\text{ex}}$ . A comparison of spectra obtained with 632.8 and 785 nm (Fig. 2) revealed a downward shift of the crystalline and amorphous diamond peaks from  $1331.2$  and  $1298\text{ cm}^{-1}$  to  $1326.9$  and  $1272\text{ cm}^{-1}$ , respectively. Similar shifts of  $\text{sp}^2$ - and  $\text{sp}^3$ -carbon bands had been observed previously in the analysis of amorphous carbon and polycrystalline diamond films over the  $\lambda_{\text{ex}}$  range 258–563 nm [20]. The possible reasons for such spectral changes might be an increase in the probing depth of the Raman experiment with a longer wavelength and the resonance enhancement of larger amorphous diamond clusters by the 785 nm excitation [6, 20, 21].

To reveal carbon structures at the BDD electrode surface, we employed surface-enhanced Raman spectroscopy (SERS) which had been successfully applied previously for the analysis of chemical vapor deposition (CVD) in diamond films [11, 14, 22, 23], diamond nanocrystals [24], highly oriented pyrolytic graphite (HOPG) [25], and amorphous carbon [26]. Before studying the BDD electrode, we had tested the purity of the Au nanoparticles deposited on the silicon substrate (Fig. 3). The broad and intense low-frequency band at  $247\text{ cm}^{-1}$ , due to the metal-adsorbate vibrational mode [27–29] (probably Au–Cl), indicates presence of colloidal Au nanoparticles at the surface. No intense bands of carbon impurities in the spectral region  $1300\text{--}1600\text{ cm}^{-1}$  were observed at the silicon surface. In contrast to the conventional Raman spectrum, an intense

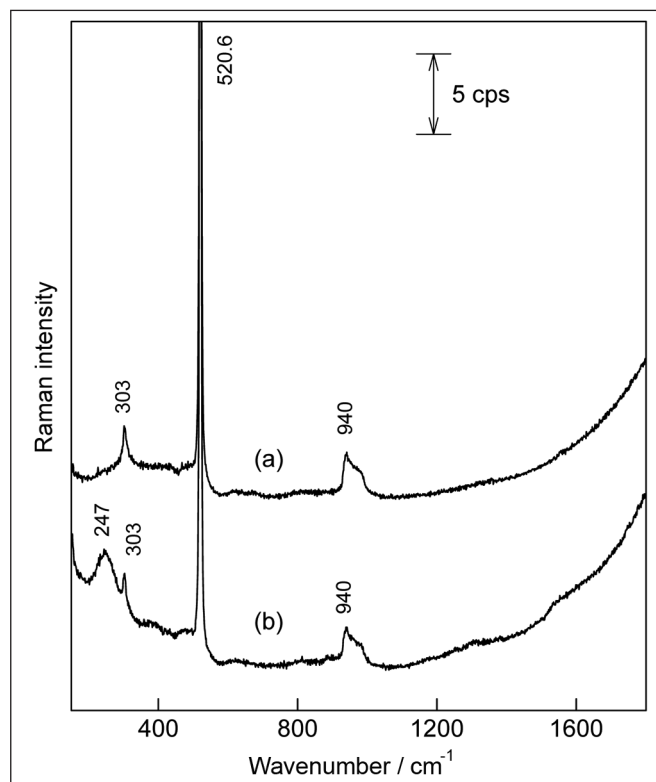


Fig. 3. Raman spectra of silicon substrate (a) without and (b) with overlayer of Au nanoparticles. Experimental conditions: integration time 500 s, excitation 785 nm, 20 mW

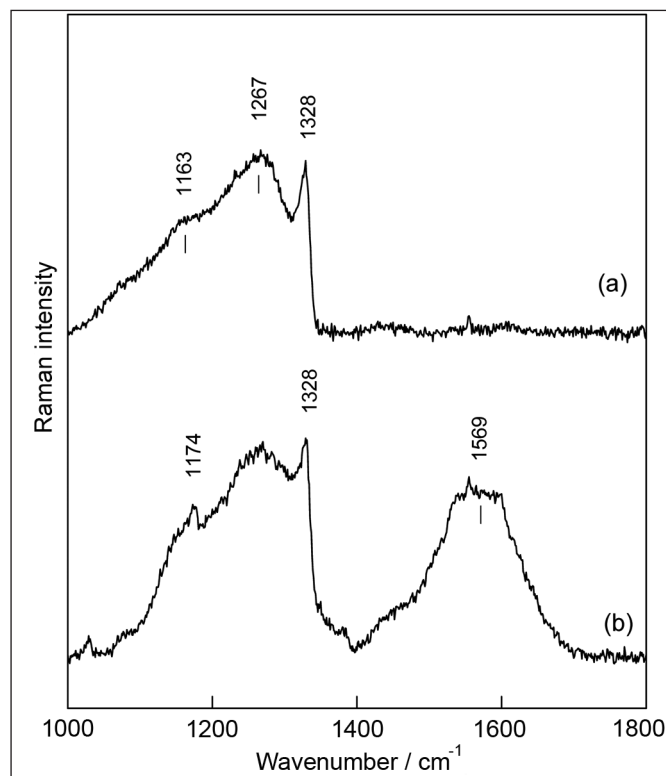


Fig. 4. Raman spectra of BDD electrode (a) without and (b) with overlayer of Au nanoparticles. Experimental conditions: integration time 500 s, excitation 785 nm, 20 mW

and broad feature in the 1500–1600  $\text{cm}^{-1}$  spectral region appears in the SERS spectrum of the BDD electrode covered with Au nanoparticles (Fig. 4). Because the frequency of the band is higher than 1330  $\text{cm}^{-1}$ , it must belong to the vibration of  $\text{sp}^2$ -structured carbon [14]. We tentatively attributed this feature to the G-band of amorphous carbon [5]. Several unresolved components compose this band, indicating presence of several structurally different  $\text{sp}^2$ -carbon segments at the interface of the BDD electrode. A similar feature had been previously detected in SERS spectra of CVD films with deposited Ag nanoparticles [14, 23]. The above SERS data show that the surface of the BDD electrode is predominantly occupied by the  $\text{sp}^2$ -like amorphous carbon as compared with the bulk structure.

## CONCLUSIONS

We have compared the Raman spectra of a boron-doped diamond electrode, obtained by using 532, 632.8, and 785 nm excitation wavelengths and demonstrated that 785-nm Raman spectrum provides information on  $\text{sp}^3$ -hybridized carbon bonds, particularly amorphous (disordered) diamond, whereas no bands of  $\text{sp}^2$ -structures associated with amorphous carbon are detected. The relative integrated intensity of the amorphous diamond band near 1274  $\text{cm}^{-1}$  with respect to the crystalline diamond peak at 1327  $\text{cm}^{-1}$  increases in the order  $1.6 < 3.3 < 7.4$  for the excitation wavelengths 532, 632.8, and 785 nm, respectively. Changes in relative intensity were found to be accompanied by a downward shift of amorphous and crystalline diamond peaks by 26  $\text{cm}^{-1}$  (1272  $\text{cm}^{-1}$  band) and 4.4  $\text{cm}^{-1}$  (1327  $\text{cm}^{-1}$  band), respectively, when the excitation wavelength was tuned from 632.8 nm to 785 nm. We have interpreted the observed spectral changes in terms of an increase in the probing depth of the Raman experiment with 785 nm and a resonance enhancement of the Raman scattering from the larger amorphous diamond clusters. We have explored the surface-enhanced Raman scattering effect to probe carbon structures at the BDD electrode surface. By depositing gold nanoparticles prepared by the hot citrate reduction method, we were able to observe a broad G band of amorphous carbon near 1569  $\text{cm}^{-1}$ , indicating the highest concentration of amorphous carbon at the BDD film surface.

## ACKNOWLEDGEMENTS

We gratefully acknowledge the Department of Bioelectrochemistry and Biospectroscopy of the Institute of Biochemistry (Vilnius) for the possibility to use the LabRam HR800 Raman spectrometer. Financial support of this project by the Lithuanian State Science and Studies Foundation (project  $2 \times \text{BioKat}$ ) is gratefully acknowledged.

Received 27 January 2009

Accepted 2 February 2009

## References

1. Y. V. Pleskov, *Russ. J. Electrochem.*, **38**, 1275 (2002).
2. M. Hupert, A. Muck, J. Wang, J. Stotter, Z. Cvackova, S. Haymond, Y. Show, G. M. Swain, *Diamond Relat. Mater.*, **12**, 1940 (2003).
3. M. Panizza, G. Cerisola, *Electrochim. Acta*, **51**, 191 (2005).
4. S. Praver, R. J. Nemanich, *Phil. Trans. R. Soc. Lond. A*, **362**, 2537 (2004).
5. D. S. Knight, W. B. White, *J. Mater. Res.*, **4**, 385 (1989).
6. J. Wagner, C. Wild, P. Koidl, *Appl. Phys. Lett.*, **59**, 779 (1991).
7. G. Niaura, A. K. Gaigalas, V. L. Vilker, *J. Raman Spectrosc.*, **28**, 1009 (1997).
8. P. Galletto, P. F. Brevet, H. H. Girault, R. Antoine, M. Broyer, *J. Phys. Chem. B*, **103**, 8706 (1999).
9. N. Wada, S. A. Solin, *Physica B*, **105**, 353 (1981).
10. A. C. Ferrary, J. Robertson, *Phys. Rev. B*, **63**, 121405 (2001).
11. T. López-Ríos, E. Sandré, S. Leclercq, E. Sauvain, *Phys. Rev. Lett*, **76**, 4935 (1996).
12. N. G. Ferreira, A. F. Azevedo, A. F. Beloto, M. Amaral, F. A. Almeida, F. J. Oliveira, R. F. Silva, *Diamond Relat. Mater.*, **14**, 441 (2005).
13. W. Windl, P. Pavone, K. Karch, O. Schütt, D. Strauch, P. Giannozzi, S. Baroni, *Phys. Rev. B*, **48**, 3164 (1993).
14. D. Roy, Z. H. Barber, T. W. Clyne, *J. Appl. Phys.*, **91**, 6085 (2002).
15. K. Ushizawa, M. N.-Gamo, K. Watanabe, I. Sakaguchi, Y. Sato, T. Ando, *J. Raman Spectrosc.*, **30**, 957 (1999).
16. P. Gonon, E. Gheeraert, A. Deneuille, F. Fontaine, L. Abello, G. Lucazeau, *J. Appl. Phys.*, **78**, 7059 (1995).
17. S. A. Solin, A. K. Ramdas, *Phys. Rev. B*, **1**, 1687 (1970).
18. N. G. Ferreira, E. Abramof, E. J. Corat, V. J. Trava-Airoldi, *Carbon*, **41**, 1301 (2003).
19. W. L. Wang, M. C. Polo, G. Sánchez, J. Cifre, J. Esteve, *J. Appl. Phys.*, **80**, 1846 (1996).
20. J. Wagner, M. Ramsteiner, Ch. Wild, P. Koidl, *Phys. Rev. B*, **40**, 1817 (1989).
21. M. Ramsteiner, J. Wagner, *Appl. Phys. Lett.*, **51**, 1355 (1987).
22. D. S. Knight, R. Weimer, L. Pilione, W. B. White, *Appl. Phys. Lett.*, **56**, 1320 (1990).
23. K. Okada, S. Komatsu, T. Ishigaki, S. Matsumoto, Y. Moriyoshi, *Appl. Phys. Lett.*, **60**, 959 (1992).
24. E. Perevedentseva, A. Karmenyan, P.-H. Chung, Y.-T. He, C.-L. Cheng, *Surf. Sci.*, **600**, 3723 (2006).
25. I. Pócsik, M. Veres, M. Füle, S. Tóth, M. Koós, *J. Non-Cryst. Sol.*, **338–340**, 496 (2004).
26. M. Veres, M. Füle, S. Tóth, M. Koós, I. Pócsik, *Diamond Relat. Mater.*, **13**, 1412 (2004).
27. A. Bulovas, Z. Talaikytė, G. Niaura, M. Kažemėkaitė, L. Marcinkevičienė, I. Bachmatova, R. Meškys, V. Razumas, *Chemija*, **18(4)**, 9 (2007).
28. A. Bulovas, N. Dirvianskytė, Z. Talaikytė, G. Niaura, S. Valentukonytė, E. Butkus, V. Razumas, *J. Electroanal. Chem.*, **591**, 175 (2006).
29. P. Gao, M. J. Weaver, *J. Phys. Chem.*, **90**, 4057 (1986).

Gediminas Niaura, Romas Ragauskas, Arvydas Dikčius,  
Benjamins Šebeka, Zenonas Kuodis

**BORU LEGIRUOTO DEIMANTO ELEKTRODO  
APIBŪDINIMAS RAMANO SPEKTROKOPIJOS  
METODU NAUDOJANT ARTIMOS INFRARAUDONO-  
SIOS SPEKTRO SRITIES (785 NM) SPINDULIUOTE**

*Santrauka*

Boru legiruotas deimanto elektrodas buvo apibūdintas įprastos Ramano spektroskopijos ir paviršiaus sustiprintos Ramano spektroskopijos metodais naudojant 785 nm lazerinę spinduliuotę. Parodyta, kad žadinant spektrus 785 nm spinduliuote, ties  $1180\text{ cm}^{-1}$  ir  $1272\text{ cm}^{-1}$  padidėja santykinis intensyvumas juostų, kurios priskirtos  $\text{sp}^3$ -hibridizacijos amorfinio deimanto virpesiams, palygin-

ti su kristalinio deimanto  $1327\text{ cm}^{-1}$  juostos intensyvumu. Be to, sumažėja amorfinio ir kristalinio deimanto juostų dažnis. Kitaip negu žadinant spektrus 532 ir 632,8 nm spinduliuotėmis, artimos infraraudonosios srities Ramano spektre nepavyko užregistruoti  $\text{sp}^2$ -hibridizacijos amorfinės anglies D ir G juostų. Pastebėti skirtumai spektruose buvo interpretuoti darant prielaidą, kad didesnio bangos ilgio Ramano eksperimentuose lazerinės spinduliuotės praskverbimo gylis padidėja, taip pat rezonansiškai sustiprėja sklaida nuo didesnių matmenų amorfinio deimanto klasterių. Darbe parodyta, kad boru legiruoto deimanto elektrodo paviršiaus anglies struktūras galima efektyviai tirti artimos infraraudonosios spektro srities paviršiaus sustiprintos Ramano sklaidos metodu naudojant Au nanodaleles, kurios buvo gaminamos įkaitinto citrato redukcijos būdu.